

METRIC GEOMETRY FOR RANKING-BASED VOTING: TOOLS FOR LEARNING ELECTORAL STRUCTURE

MOON DUCHIN AND KRISTOPHER TAPP

ABSTRACT. In this paper, we develop the metric geometry of ranking statistics, proving that the two major permutation distances in the statistics literature—Kendall tau and Spearman footrule—extend naturally to incomplete rankings with both *coordinate embeddings* and *graph realizations*. This gives us a unifying framework that allows us to connect popular topics in computational social choice: metric preferences (and metric distortion), polarization, and proportionality.

As an important application, the metric structure enables efficient identification of *blocs* of voters and *slates* of their preferred candidates. Since the definitions work for partial ballots, we can execute the methods not only on synthetic elections, but on a suite of real-world elections. This gives us robust clustering methods that often produce an identical grouping of voters—even though one family of methods is based on a Condorcet-consistent ranking rule while the other is not.

CONTENTS

1. Introduction	2
1.1. Related work	3
2. Ballot graphs and coordinate embeddings	3
2.1. Coordinate embeddings	3
2.2. Ballot graphs	4
2.3. Generalized ballot graphs	6
2.4. Relating the ballot graphs to coordinate embeddings	7
2.5. Relating the generalized ballot graph to coordinate embeddings	9
3. Finding blocs and slates; synthetic validation	10
3.1. Grouping the ballots	10
3.2. Grouping the candidates	11
3.3. Synthetic elections	12
4. Results on Scottish elections	14
4.1. Learning voter blocs in Pentland Hills	14
4.2. Learning candidate slates in Pentland Hills	15
4.3. Overview across dataset	16
5. Conclusion	17
Acknowledgements	17
References	18
Appendix A. Comparing heuristic methods	20
Appendix B. Visualizing polarization	21

2020 *Mathematics Subject Classification.* Primary 05C12; Secondary 91B12, 91B14.

Key words and phrases. ranking statistics, permutation distances, metric geometry, computational social choice, ballot clustering.

1. INTRODUCTION

A major research direction in computational social choice theory has been the study of metric preferences: both candidates and voters are thought to be embedded in a common (unobserved) metric space, and the “cost” of a candidate is the sum of their distances to the voters. In this framework, each metric embedding has an optimal winner (the lowest-cost candidate); however, many metrics are consistent with a given preference profile that records the ordinal preferences of the voters, and the identity of the optimal winner may vary. Numerous works have studied the *metric distortion* for voting rules, defined as the worst-case cost ratio over all metric realizations.

A second strand of research has aimed to provide descriptive measures of preference, such as by measuring the level of *polarization* for a ranked choice election, the level of preference *diversity*, or the degree of *proportionality* for multi-winner elections. All of these have natural interpretations in the metric framework presented here.

The purpose of this paper is to build out the metric theory for elections, not through a worst-case analysis but by a close study of two choices of metric. As an application, we obtain natural methods for grouping similar voters and candidates, respectively, and identifying them as voter *blocs* and candidate *slates*. We test the methods on synthetic preference profiles and on a real-world dataset of over 1000 ranked-choice local government elections in Scotland from 2012 to 2022, which feature five major parties and dozens of minor ones. Because our methods do not make use of party labels, we are able to identify patterns that might be otherwise missed by party-focused analysis.

By a *ballot*, we mean a complete or partial ranking of m candidates. (In places, we also consider the fuller setting of weak rankings, allowing arbitrary ties.) We will introduce coordinate embeddings that correspond to the two most important notions of ranking distance in the statistics literature, defined for complete and partial ballots. A *preference profile* is a finite set of ballots.

The first metric embedding assigns a ballot to a point in \mathbb{R}^m by taking each candidate’s coordinate to be the reverse of their ranking, so that a candidate earns a score of $m - j$ from a voter who ranks them j th. Because this system of scoring is sometimes called (standard) *Borda points* in the context of voting, we call this the *Borda embedding*. An alternative system of coordinates maps a ballot to $\{-1, 0, 1\}^{\binom{m}{2}} \subset \mathbb{R}^{\binom{m}{2}}$, where each pairwise comparison is recorded as favoring one of the two candidates (± 1) or as a tie (0). We call this the *head-to-head embedding*. We then define the distances d_B and d_H between ballots as half the L^1 distance between the corresponding vectors. These recover Spearman footrule and Kendall tau (also known as swap distance, or bubble sort distance), respectively. A preference profile sits as a point cloud in the associated coordinate space. An optimal center under the L^1 metric in the head-to-head embedding is precisely the Kemeny ranking, and k -clustering in this setting is the k -Kemeny problem. In the Borda embedding, it is the L^2 minimizer that would recover the usual Borda ranking rule—the coordinates record average Borda score for candidates. L^1 minimizers give a Borda median ranking; this has been studied under the heading of rank aggregation but not fully embraced in social choice theory as a voting rule.

As an alternative to coordinate embeddings, we realize d_B and d_H as graph metrics. We define a sparse graph called the *ballot graph* whose nodes are partial rankings and whose path metric recovers d_H ; by adding edges, we obtain a *shortcut ballot graph* that recovers d_B .

There are several main contributions, including: **Extension of metric results.** Not only complete rankings, but partial rankings, candidates, and slates all receive assigned locations in a common space. **Graph realizations.** We build graphs that incorporate partial rankings, with results connecting them to the principal ranking metrics (Kendall and Spearman). Notably, the Borda graph realization works with some partial-ballot conventions and not others. **Empirical methods.** The incorporation of partial ballots lets us deploy our methods on real elections. We use both synthetic and real-world elections for validation, and show empirical robustness to modeling choices.

Sometimes, the extension of complete-ranking results to partial rankings can be done with essentially routine constructions. But that is not the case here, where the arguments are far from trivial and the extension to partial rankings forces certain choices that are not obvious; this can be thought of as revealing structure that was already present in the setting of full permutations.

Overall, we develop fundamental tools in the geometry of rankings, apply these tools to the unsupervised learning problem of detecting blocs and slates, and show that we get stable and interpretable results. All data and code used in this paper are available at <https://github.com/mggg/ballot-clustering>

1.1. Related work. Well-studied metrics on full permutations (i.e., complete ballots) include the *Spearman footrule* and the *Kendall tau distance* Kendall [1970], Kendall and Gibbons [1990]. The classic paper of Diaconis and Graham [1977] calls them D and I , respectively, and establishes that the two metrics are mutually bounded. These agree with our metrics via $d_H = I$ and $d_B = \frac{1}{2}D$. In our notation, the (sharp) bounds are $\frac{1}{2}d_H \leq d_B \leq d_H$. The same bounds were generalized to partial permutations of fixed length (that is, top- k rankings) by Fagin et al. [2003] and then to more general ballots by a larger set of co-authors in Fagin et al. [2006]. These papers employ the *averaged* Borda convention for ballots that are short or allow general ties, awarding the candidates in a tied ranking the average of the Borda points they would receive in any resolution of ties. We consider an alternative, sometimes called the *pessimistic* Borda convention, that awards the fewest points over all resolutions—i.e., zero points for all unmentioned candidates Kamwa [2022]. Not only do the Diaconis–Graham bounds extend to pessimistic Borda distance on partial ballots, but that metric is well adapted to a sparse graph realization, whereas averaged Borda is not. The idea of a ballot graph has been used by several authors; see for example the beautiful illustrations in Puppe [2018]. However, to our knowledge, previous work is limited to d_H distances between complete ballots.

An application of these metrics in the literature that closely aligns with our centroid-based clustering methods is what is known as the *rank aggregation* problem. In the context of rank aggregation, the center is required to be a full ranking (whose summed distance to the input rankings is minimized) and is viewed as "consensus" ranking Dwork et al. [2001], Van Zuylen and Williamson [2009], so that rank aggregation can be viewed as a voting method. For example, Fishburn [1977] explores which Arrow-style axioms are satisfied by various methods of rank aggregation. In our work, we find it productive to use a slightly different interpretive framework: the center of each cluster is a useful summary statistic of the voting behavior within that cluster, whether or not it is a ranking and whether or not the voters are closely concentrated nearby.

We connect to the extensive literature on metric preferences and distortion in social choice, surveyed in Anshelevich et al. [2021]. The identification of blocs and slates will give strong grounding for the measurement of proportionality, diversity, and polarization, which are topics of longstanding interest (and current activity) in computational social choice Skowron et al. [2017], Israel and Brill [2025], Hashemi and Endriss [2014], Karpov [2017].

For *polarization* in particular, axiomatic developments are found in classic economics papers like Esteban and Ray [1991] and Can et al. [2015]. The work most closely aligned with ours is Faliszewski et al. [2023], whose authors define diversity and polarization indices for an election (with complete rankings) in terms of the k -clusterings that minimize the ballots' summed d_H -distances to k centers. With our tools, their definitions can be extended to partial ballots and executed at scale. The authors of Busse et al. [2007] cluster the ballots of an election by fitting the parameters of a Mallows model. By contrast, we identify clusters without assuming that the ballots follow any particular distribution.

2. BALLOT GRAPHS AND COORDINATE EMBEDDINGS

Let Ω_m be the set of possible partial or complete ballots in an election with m candidates. The candidates can be denoted $\{A, B, \dots\}$ or $\{A_1, \dots, A_m\}$. We will adopt flexible notation for ballots, so that

$$(A, C, D, B), \quad A > C > D > B, \quad ACDB, \quad \text{and} \quad \begin{pmatrix} A \\ C \\ D \\ B \end{pmatrix}$$

all denote the same ballot. We will record partial ballots as having unmentioned candidates tied at the end of the ballot, so that (A, B) or $(A, B, -, -)$ is identified with $(A, B, \{C, D\})$. Partial ballots therefore only allow ties at the end of the ballot; *generalized ballots* would allow ties in arbitrary positions.

2.1. Coordinate embeddings.

Definition 2.1 (Borda and head-to-head distance). Suppose σ is a permutation of the symbols $1, \dots, m$, with the convention that σ maps a candidate index to the rank of that candidate on the ballot, i.e., for candidates A_1, \dots, A_m , we have that $\sigma(i)$ is the position in which the voter ranked A_i . In this notation, the

ranking corresponding to σ is $\begin{pmatrix} \sigma^{-1}(1) \\ \vdots \\ \sigma^{-1}(m) \end{pmatrix}$.

Extend this to partial ballots by the *pessimistic* convention: if j is an unlisted candidate, then $\sigma(j) = m$. In places, we will also refer to the *averaged* convention whereby $\sigma(j)$ equals the average of the rankings that

all of the unlisted candidates would have received if they had been ranked. Averaging maintains the total sum of ranks for any ballot, complete or partial, as $\sum_i \sigma(i) = \binom{m+1}{2}$, while the pessimistic convention lets that sum vary—in other words, embedding with the averaged convention sends all ballots onto a common hyperplane.

Define functions $\mathbf{b} : \Omega_m \rightarrow \mathbb{R}^m$ and $\mathbf{h} : \Omega_m \rightarrow \mathbb{R}^{\binom{m}{2}}$ by

$$\mathbf{b}(\sigma)(i) = m - \sigma(i), \quad \mathbf{h}(\sigma)(\{i, j\}) = \begin{cases} +1 & \sigma(i) > \sigma(j) \\ 0 & \sigma(i) = \sigma(j) \quad (\text{assuming } i < j) \\ -1 & \sigma(i) < \sigma(j) \end{cases}$$

Then the Borda distance and head-to-head distance are defined by

$$d_B(\sigma, \tau) = \frac{1}{2} \|\mathbf{b}(\sigma) - \mathbf{b}(\tau)\|_1, \quad d_H(\sigma, \tau) = \frac{1}{2} \|\mathbf{h}(\sigma) - \mathbf{h}(\tau)\|_1.$$

Example 2.2. In Ω_4 , the ballot AD is mapped to the Borda point $(3, 0, 0, 2)$. Since the 6 head-to-head comparisons are AB, AC, AD, BC, BD, CD , the ballot AD has the head-to-head image $(1, 1, 1, 0, -1, -1)$.

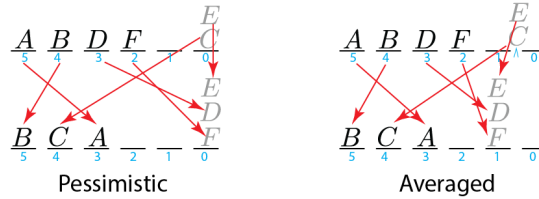


FIGURE 1. Under the pessimistic convention, the total shifts to convert (A, B, D, F) to (B, C, A) sum to 12, while they sum to 10 in the averaged convention; the Borda distances would be 6 and 5, respectively.

Rank differences can be visualized as positional shifts, as illustrated in Figure 1.

The head-to-head embedding uses an order on candidates, whether alphabetical or an arbitrary fixed order, and the value $+1$ means that the first-indexed candidate is ranked higher. For complete ballots, d_H is exactly the Kendall tau distance, counting neighbor swaps between permutations; for short ballots, d_H agrees with the generalization of the Kendall tau metric discussed in Fagin et al. [2006].

2.2. Ballot graphs. Any finite metric space can be given a graph realization in a trivial way: by adding an edge between each pair x, y of vertices with weight $d(x, y)$. (The triangle inequality ensures that the path metric on that graph is d .) Thus, for a graph realization to add value, it should be relatively sparse in terms of the edges needed to recover the metric as the path metric. In this section we introduce *ballot graphs* that are sparse in the sense that, though the number of nodes will grow as roughly $2m!$ for the graph on m candidates, the degree of each vertex will be only polynomial in m .

Definition 2.3 (Ballot graphs). The *ballot graph* \mathcal{G}_m is a weighted, undirected graph with possible ballots as the vertex set ($V = \Omega_m$). Since we treat unmentioned candidates as being tied at the end of a ballot, we will identify each ballot of length $m - 1$ with its extension to a complete ballot. There are two types of edges.

- Neighbor swaps: $(\sigma, \tau) \in E$ whenever $\sigma^{-1}\tau$ is an adjacent transposition $(i, i + 1)$. These edges are given unit weight.
- Truncation and extension: when σ and τ have length $k - 1$ and k and agree in the first $k - 1$ positions, then $(\sigma, \tau) \in E$ is given weight $\frac{m-k}{2}$.

The *shortcut ballot graph* \mathcal{G}_m^+ adds a more general swap edge.

- General swaps: $(\sigma, \tau) \in E$ when $\sigma^{-1}\tau$ is a transposition $(i, i + k)$ for some i, k , and its weight is set to k . In other words, these edges correspond to swaps of candidates in not-necessarily-successive positions, at a cost that is equal to the difference in rank.

Note that neighbor swaps are a special case of general swaps. We will use the notions of edge weight, edge length, and the "cost" of a move interchangeably. Treating edge weights as lengths lets us study the induced path metric: the distance between two ballots is equal to the length of the shortest edge-path between them.

Example 2.4 (Illustrating ballot graph construction).

- The ballot graph \mathcal{G}_3 is shown in Figure 2. For instance, the distance from ABC to ACB is one because they differ by a neighbor swap.
- In \mathcal{G}_4 (Figure 3), the distance from $ABCD$ to its reversal $DCBA$ equals 6. Note that this can either be realized through a path of 6 neighbor swaps or through a path that goes through bullet votes:

$$ABCD \rightarrow ABC \rightarrow AB \rightarrow A \rightarrow AD \rightarrow DA \rightarrow D \rightarrow DC \rightarrow DCB \rightarrow DCBA.$$

(That these two kinds of paths have equal length generalizes to connecting any complete ballot and its reversal in any \mathcal{G}_m .) In \mathcal{G}_4^+ , the distance drops to 4 with the use of a shortcut edge $ABCD \rightarrow DBCA$, whose length is 3, plus one additional neighbor-swap.

- In \mathcal{G}_6 , the edge from (A, B) to (A, B, C) has weight $\frac{3}{2}$.

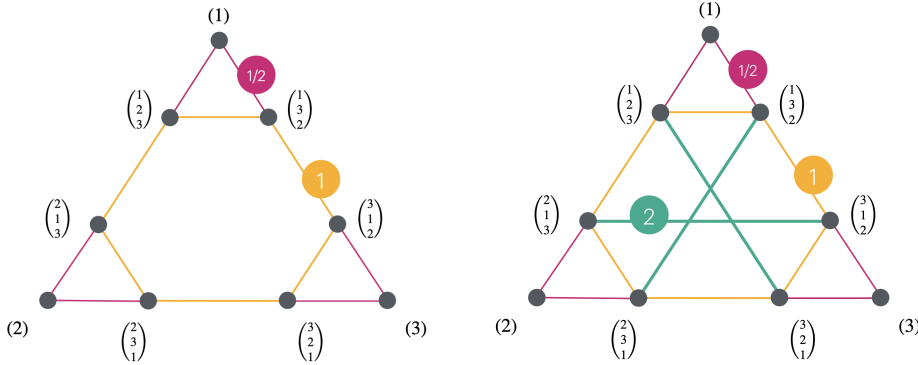


FIGURE 2. The basic ballot graph \mathcal{G}_3 and shortcut ballot graph \mathcal{G}_3^+ . Swaps of the first and last place correspond to new edges of length 2, providing shortcuts between nodes that would otherwise be 3 apart.

Proposition 2.5. *In either \mathcal{G}_m or \mathcal{G}_m^+ , size of the vertex set is $O(m!)$ and the degree of each vertex is $O(m^2)$.*

Proof. The number of complete or partial rankings of m objects, including the empty ranking, is $\lfloor em! \rfloor$. This can be seen by counting partial rankings as $\sum_{k=0}^m \frac{m!}{(m-k)!} = m! \sum_{j=0}^m \frac{1}{j!}$ and comparing to $e = \sum_{j=0}^{\infty} \frac{1}{j!}$.

Because we identify ballots of length m with their truncations of length $m-1$, the number of vertices grows like $(e-1)m!$. If a vertex represents a ballot of length $1 < k < m-1$, it has one neighbor by truncation, $m-k$ neighbors by extension, and $k-1$ swap neighbors, giving degree m in \mathcal{G}_m . Complete ballots have one neighbor by truncation (of length $m-2$) and $m-1$ swap neighbors, for the same degree. Bullet votes have $m-1$ extensions; if we include the empty ballot in the graph, their degree is also m (making \mathcal{G}_m an m -regular graph), and otherwise it is $m-1$.

In the shortcut graph, the number of swap neighbors for the ballot of length k is $\binom{k}{2}$ instead of $k-1$, which contributes less than $\frac{1}{2}m^2$ to the degree. \square

These graphs extend important mathematical objects that occur in group theory and combinatorics. Restricting \mathcal{G}_m to the complete ballots recovers the Cayley graph of the symmetric group S_m (with standard transposition generators), which shows up in Figure 2 as a 6-cycle in \mathcal{G}_3 . Adding shortcut edges amounts to adding additional generators. Another way to phrase this is that the 1-skeleton of the permutohedron—a polytope used to track the structure of permutations—sits in each \mathcal{G}_m . Using this kind of mathematical structure allows us to phrase the results of elections as distributions on a graph or network.¹

¹There are many deep open questions about these: for instance, the Babai conjectures relate to diameter bounds and spectral gaps for Cayley graphs of S_m as the generators vary.

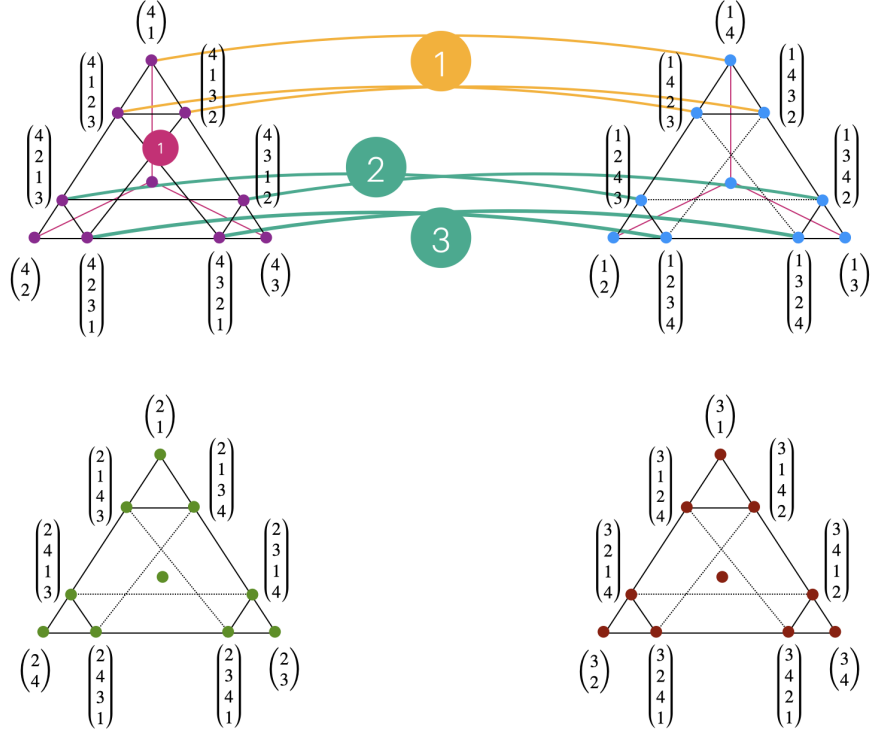


FIGURE 3. An illustrative portion of the shortcut ballot graph \mathcal{G}_4^+ , showing the connections between ballots headed by candidates 4 and 1. The construction of this picture shows the recursion $|\Omega_m| = m \cdot |\Omega_{m-1}| + m$.

2.3. Generalized ballot graphs. Next, consider the case that ballots are allowed to include general ties. For example, with 7 candidates, the *generalized ballot*

$$(C, \{A, D\}, \{B, F, G\}, E)$$

reflects equal preference for A and D , and for B , F , and G . This allows us to write a preference between slates: if $\mathcal{C} = \mathcal{A} \sqcup \mathcal{B}$ is a partition of the set \mathcal{C} of candidates into slates, then the preference $\mathcal{A} > \mathcal{B}$ can be considered as a generalized ballot. Without loss of generality, every candidate appears once in a generalized ballot; complete and partial ballots are both special cases, since partial ballots were already interpreted as having a tie in the last position. Let $\tilde{\Omega}_m$ denote the set of generalized ballots in an election with m candidates.

The *generalized ballot graph* $\tilde{\mathcal{G}}_m$ is a graph on these nodes. There is an edge between two nodes whenever one ballot is obtained from the other by merging the candidate sets in adjacent positions, and the length of that edge is $\frac{1}{2}$ times the product of their orders. This simple edge rule correctly generalizes both edge rules for \mathcal{G}_m .

Example 2.6. The graph $\tilde{\mathcal{G}}_4$ contains the unit-length path

$$(A, B, C, D) \xrightarrow{5} (A, \{B, C\}, D) \xrightarrow{5} (A, C, B, D).$$

Swapping any pair of adjacent singleton candidates similarly has cost 1.

We enlarge the domain of \mathfrak{h} to $\tilde{\mathcal{G}}_m$ accordingly: as before, its $\binom{m}{2}$ coordinates represent ordered pairs of candidates, and the value of each coordinate is -1 (lose), 0 (tie), or 1 (win). Here a tie means that the candidates belong to the same candidate set.

Note that these generalized ballot graphs have a super-factorial number of nodes (counted by the Fubini numbers) and now have exponentially growing degree. That is because each generalized ballot has at most

$m - 1$ ways to merge neighboring candidate sets, but if a candidate set has k elements then there are 2^k ways to split it, so for instance a bullet vote has many neighbors.

2.4. Relating the ballot graphs to coordinate embeddings.

Theorem 2.7 (Graphs match L^1 distances). *The distance d_H is realized as the path metric on the basic ballot graph \mathcal{G}_m , while d_B is realized as the path metric on the shortcut ballot graph \mathcal{G}_m^+ .*

To prove this, it is convenient to introduce notions of strong and weak disagreement. We say that ballots σ, τ have a strong disagreement on candidates i, j if one candidate is ranked higher on σ while the other is ranked higher on τ ; a weak disagreement occurs when one ballot expresses a preference where the other ballot records a tie. Then for a pair of ballots σ, τ we can define $\text{str}(\sigma, \tau)$ and $\text{wk}(\sigma, \tau)$ as the total number of strong and weak disagreements, respectively. For example, if $\sigma = (A, B, C)$ and $\tau = (A, E)$ in Ω_5 , then $\text{str}(\sigma, \tau) = 2$ and $\text{wk}(\sigma, \tau) = 4$. Since a strong disagreement occurs when a coordinate of the head-to-head vector is $+1$ in one ballot and -1 in the other, it contributes 2 to the L^1 difference; similarly, a weak disagreement contributes 1. It is therefore immediate that

$$d_H = \text{str} + \frac{1}{2} \text{wk}$$

for any pair of ballots. To prove that the graph distance matches d_H , it suffices to describe graph distance in terms of strong and weak disagreements.

Proof. We begin with d_H . For a pair of ballots σ, τ that are adjacent in \mathcal{G}_m , we verify that the weight of the edge between them equals $w(\sigma, \tau) = \text{str} + \frac{1}{2} \text{wk} = d_H(\sigma, \tau)$ by checking the cases of neighbor-swap and extension. Now consider a geodesic in \mathcal{G}_m visiting vertices $\sigma_1, \dots, \sigma_r$ and note that the graph distance equals $\sum w(\sigma_i, \sigma_{i+1})$ by definition of geodesic. On the other hand, $d_H(\sigma_1, \sigma_r)$ is less than or equal to this sum, because d_H is defined as an L^1 difference, so it satisfies the triangle inequality. Thus d_H is less than or equal to the graph distance.

To show that this is an equality, we construct a path realizing the distance equality between arbitrary ballots σ, τ . To do this, we construct "waypoints": if σ is a partial ballot, let σ' be the possibly longer ballot which agrees with σ on all listed candidates, then ranks candidates that were mentioned in τ but not σ in the order in which they appear in τ ; likewise, τ' starts like τ but adds missing candidates in the order of appearance in σ .

Consider the path from σ to σ' via extensions, continuing to τ' by a minimal sequence of neighbor swaps, then extending to τ by truncation. To see that this suffices, note that for two distinct ballots that are complete (or more generally that have the same candidate set), there must be at least one neighboring pair of candidates that witnesses the strong disagreement. Otherwise, every X ranked above Y by the first ballot would also be ranked above Y by the second ballot, forcing the ballots to be identical. This means that there is always a neighbor swap that reduces the strong disagreement count by 1, until that count is zero. Thus the length of the path $\sigma' \rightarrow \tau'$ is $\text{str}(\sigma, \tau)$.

Suppose there are k candidates mentioned in τ but not σ and l candidates mentioned in neither ballot. Then the path distance from σ to σ' is $\frac{l+\dots+(l+k)}{2} = \frac{1}{2} \left(\binom{k}{2} + kl \right)$. The number of weak disagreements involving those candidates is $\binom{k}{2} + kl$. Similarly between τ and τ' the total edge weight is one-half of the number of weak disagreements involving candidates unmentioned in τ but mentioned in σ . Taken together, we've shown that the natural path $\sigma \rightarrow \sigma' \rightarrow \tau' \rightarrow \tau$ has total edge weight $\text{str}(\sigma, \tau) + \frac{1}{2} \text{wk}(\sigma, \tau)$, as desired.

Next, to prove that $d_B(\sigma, \tau)$ equals the path distance in \mathcal{G}_m^+ , we use the same waypoints σ', τ' and the same path segments $\sigma \rightarrow \sigma'$ and $\tau \rightarrow \tau'$, whose lengths also realize the d_B -distance.

It remains to construct a d_B -geodesic $\sigma' \rightarrow \tau'$ in \mathcal{G}_m^+ ; that is, a path in \mathcal{G}_m^+ that realizes the d_B distance. Note that a path from σ' to τ' is a d_B -geodesic if and only if each candidate's Borda score changes monotonically between its starting score in σ' and ending score in τ' . From its position in σ' , every candidate needs to shift either to a lower position (\downarrow), higher (\uparrow) or neither (\square) to reach its target position in τ' . We represent this as a *state vector* as in Figure 4. We proceed in steps, each time swapping the candidates corresponding to the first \uparrow symbol and the last \downarrow symbol before it. Repeating this process until reaching τ' produces a Borda geodesic because each candidate can only move toward its target position; the move never overshoots the target position because the candidates in between those who swapped were already in their final positions. \square

σ	σ'	$\tau' = \tau$	
	$A \downarrow$	$A \downarrow$	$D \square$
A	$C \square$	$C \square$	C
C	$B \downarrow$	$D \uparrow$	$A \square$
B	$D \uparrow$	$B \downarrow$	$B \downarrow$
E	\uparrow	$E \uparrow$	$E \uparrow$

FIGURE 4. For ballots $\sigma = (A, C, B)$ and $\tau = (D, C, A, E, B)$, we first complete σ to σ' and then make swaps as indicated (in red) for a total Borda distance of $d_B(\sigma', \tau') = 1 + 2 + 1 = 4$. This correctly matches half the L^1 difference of $\mathbf{b}(\sigma') = (4, 2, 3, 1, 0)$ and $\mathbf{b}(\tau') = (2, 0, 3, 4, 1)$.

Remark 2.8. This proof fails for the averaged Borda convention. With the pessimistic convention, moving a candidate from σ out of a tie at the end does not change the position of the remaining unmentioned candidates, so it moves σ closer to σ' . But under averaging, the extension move can improve the position of one candidate but worsen the position of others.

In fact, a simple example of this kind suffices to show that our local moves are not enough to realize averaged Borda with graph distance. Consider what is needed to transform a bullet vote for A to a bullet vote for B when there are many candidates. In the averaged convention, all other candidates have the same Borda score in the initial and terminal ballot. But extending A to AB changes the average score of the others, and we easily see that a direct edge from A to B would be needed. Similar arguments force an explosion of degree.

The following is a simple application of the strong and weak disagreement count.

Proposition 2.9. $d_H(\sigma, \tau)$ equals the average (over all extensions of σ and τ to complete ballots) of the number of adjacent swaps needed to convert σ into τ .

Proof. If σ or τ is an incomplete ballot, then randomly completing them resolves each weak disagreement into either an agreement or a strong disagreement, with equal likelihood. Thus, the expected number of strong disagreements between their completions equals $\text{str} + \frac{1}{2} \text{wk}$. \square

Theorem 2.10.

$$\frac{1}{2} \text{str} + \frac{1}{2} \text{wk} < d_B \leq \text{str} + \frac{1}{2} \text{wk} = d_H$$

Proof. The proof of Theorem 2.7 established that

$$d_B(\sigma, \tau) = \underbrace{d_B(\sigma, \sigma') + d_B(\tau, \tau') + d_B(\sigma', \tau')}_{{= \frac{1}{2} \text{wk}(\sigma, \tau)}},$$

so it remains to show that $d_B(\sigma', \tau')$ (which is the \mathcal{G}_n^+ -path distance between σ' and τ') is more than half $\text{str}(\sigma', \tau')$ (which is the \mathcal{G}_n -path distance). For this, it will suffice to prove that the weight of each shortcut edge of \mathcal{G}_n^+ is more than half the \mathcal{G}_n -distance between its endpoints. Every shortcut edge of length k represents two candidates jumping over $k - 1$ stationary candidates located in between them; with neighbor swaps, this can be realized by moving the lower candidate k spots and the higher candidate $k - 1$ spots, for $2k - 1$ overall. Thus each shortcut speeds up a path segment by a factor less than two. \square

Corollary 2.11. $d_B \leq d_H < 2d_B$.

Fagin et al. [2006] define a family of metrics they denote by $K^{(p)}$ as $\text{str} + p \cdot \text{wk}$, so that $d_H = K^{(1/2)}$. They prove that these are true metrics on the space of ballots with arbitrary ties when $p \in [1/2, 1]$, and that they are "near-metrics" (satisfying a relaxed triangle inequality) for $p \in (0, 1/2)$.

Remark 2.12. The Borda distance d_B is not a multiple of any $K^{(p)}$. To see this, note that complete ballots have no weak disagreements. So for d_B to be a rescaling of some $K^{(p)}$ on complete ballots, it would have to be proportional to the number of strong disagreements. Consider $\sigma = ABCDE$, $\tau = EBCDA$, and $\pi = DBCAE$. The candidate swap with rank difference four means ballot τ requires 7 inversions to convert to σ while their shortcut edge has length 4; the swap three units apart means π vs. σ needs 5 inversions

while their shortcut edge has length 3. This shows that d_B is not a fixed multiple of str , so $d_B \neq a \cdot \text{str} + b \cdot \text{wk}$ for any a, b .

The next result is shown by Fagin et al. for averaged Borda, and also holds for our (pessimistic) d_B .

Corollary 2.13. *For any pair $\sigma, \tau \in \Omega_n$ of distinct ballots, $\frac{d_H(\sigma, \tau)}{d_B(\sigma, \tau)} \in [1, 2]$, and these bounds are sharp.*

Proof. The bound is just a rephrasing of Corollary 2.11, so it remains to establish optimality. If $\sigma \in \Omega_m$ is a complete ballot, let $\hat{\sigma}$ be its reversal, with candidates listed in opposite order. We have $d_H(\sigma, \hat{\sigma}) = \binom{m}{2}$ because every pair will have a strong disagreement. On the other hand, $d_B(\sigma, \hat{\sigma}) = (m-1)(m+1)$, so comparing these gives a sequence with $\frac{d_H(\sigma, \hat{\sigma})}{d_B(\sigma, \hat{\sigma})} \rightarrow 2$. For the other bound, just note that any pair of ballots connected by a single neighbor swaps realizes $d_H = d_B$. \square

In the proof of Theorem 2.10, we noted that a shortcut edge of length k replaces a path of length $2k-1$ in the basic ballot graph. This means its distance savings is $k-1$. Thus if the shortcut edges used in a geodesic have lengths k_1, k_2, \dots, k_r , we have the exact accounting $d_H - d_B = (\sum k_i) - r$.

For complete ballots in S_m , Diaconis and Graham show that the expected Kendall tau distance to the identity is $I = m^2/4$ and the expected Spearman footrule distance is $D = m^2/3$ [Diaconis and Graham, 1977, Table 1]. Since $d_H = I$ and $d_B = \frac{1}{2}D$, this gives that the average value of d_H is $3/2$ the average value of d_B .

As a final remark on natural ways to metrize the space of ballots, note that we can regard a ballot with ties as a collection of all complete ballots obtained by arbitrary resolution of ties. Rather than computing the average as in Proposition 2.9, one could measure the maximum or the minimum distance between points in the resolution of one ballot to those representing the other. In Critchlow [1985], Critchlow also studied the Hausdorff distance between these point clouds $\bar{\sigma}$ and $\bar{\tau}$, namely the smallest ϵ so that the ϵ -neighborhood of $\bar{\sigma}$ contains $\bar{\tau}$, and likewise the ϵ -neighborhood of $\bar{\tau}$ contains $\bar{\sigma}$, with respect to swap distance. Fagin et al. [2006] proved the following characterization. Let σ, τ be partial ballots and define $\text{wk}(\sigma \rightarrow \tau)$ to be the number of candidates mentioned in τ but not σ while $\text{wk}(\tau \rightarrow \sigma)$ is the reverse, so that $\text{wk}(\sigma, \tau)$ is the sum of these two asymmetric values, then

$$d_{\text{Haus}}(\sigma, \tau) = \text{str}(\sigma, \tau) + \max(\text{wk}(\sigma \rightarrow \tau), \text{wk}(\tau \rightarrow \sigma)).$$

Because the max of two numbers is no greater than their sum but no less than half of their sum, we get $d_H \leq d_{\text{Haus}} \leq 2d_B$.

2.5. Relating the generalized ballot graph to coordinate embeddings. Between a pair of generalized ballots, we define weak and strong disagreements exactly as before; in particular, a pair of ballots has a weak disagreement between two candidates if the candidates tie (are in the same ranking position) with respect to exactly one of the two ballots. Just like before, we define

$$d_H(\alpha, \beta) = \frac{1}{2} \|\mathbf{h}(\alpha) - \mathbf{h}(\beta)\|_1$$

for all $\alpha, \beta \in \tilde{\Omega}_m$, and we observe that

$$d_H(\alpha, \beta) = \text{str}(\alpha, \beta) + \frac{1}{2} \text{wk}(\alpha, \beta).$$

A portion of Theorem 2.7 generalizes as follows.

Proposition 2.14. *The path metric on $\tilde{\mathcal{G}}_m$ realizes d_H on generalized ballots.*

Proof. To start, let's define the common refinement of two generalized ballots. It is the coarsest grouping of candidates so that two candidates appear together in the common refinement iff they are grouped together in both ballots. For instance, the common refinement of $(A, \{B, C\}, D, \{E, F\})$ and $(\{B, D\}, \{A, C\}, \{D, E, F\})$ consists of A, B, C, D singletons and the pair $\{E, F\}$.

Next, note that the edges in $\tilde{\mathcal{G}}$ are defined as merges of candidate sets ranked in neighboring positions. Recall that if one set has r candidates and the neighboring set has s candidates, then the edge between them was given length $rs/2$. Also note that the ranking that had them separate had rs strong preferences among those candidates, while the ranking that has them all grouped has only weak preferences.

For a pair $\alpha, \beta \in \tilde{\Omega}_m$, we must construct a path from α to β in $\tilde{\mathcal{G}}_m$ whose edge weights sum to the weighted disagreement count. We design such a path with waypoints

$$\alpha \rightarrow \alpha' \rightarrow \beta' \rightarrow \beta,$$

where α' and β' resolve all ties from their respective ballots that are not present in the common refinement. To resolve such a tie in α , we use the strict preference seen in β , and vice versa. Thus α' and β' both have the common refinement as their candidate sets. Then we can see that the path distance $\alpha \rightarrow \alpha'$ plus the distance from $\beta \rightarrow \beta'$ uses moves that resolve a single weak disagreement between α and β and each such move requires a path of length $1/2$, so those lengths sum to $\frac{1}{2} \text{wk}(\alpha, \beta)$.

On the other hand, every step in the path $\alpha' \rightarrow \beta'$ only resolves strong disagreements, so its lengths sum to $\text{str}(\alpha, \beta)$. \square

The shortcut constructions for d_B and $d_{B_{\text{avg}}}$ (pessimistic and averaged conventions, respectively) generalize cleanly to $\tilde{\Omega}_m$, with the Borda conventions applied within each candidate set in the corresponding way.

Fagin et al. [2006] prove that the previous distance bounds extend to generalized ballots under the averaged convention.

Proposition 2.15. *If $\alpha, \beta \in \tilde{\Omega}_m$ are distinct, then $\frac{d_{B_{\text{avg}}}(\alpha, \beta)}{d_H(\alpha, \beta)} \in [1, 2]$.*

However, the corresponding statement is false for d_B .

Example 2.16. If $\alpha = (\{A_1, \dots, A_k, \textcolor{red}{X}\}, \{B, \textcolor{red}{Y}\})$ and $\beta = (\{A_1, \dots, A_k, \textcolor{red}{Y}\}, \{B, \textcolor{red}{X}\})$ in $\tilde{\Omega}_{k+3}$, then we have $d_B(\alpha, \beta) = 4$ and $d_H(\alpha, \beta) = 2 + k$, so $\lim_{k \rightarrow \infty} \frac{d_B(\alpha, \beta)}{d_H(\alpha, \beta)} = 0$.

3. FINDING BLOCS AND SLATES; SYNTHETIC VALIDATION

3.1. Grouping the ballots. Once the ballots are given coordinate representations by the Borda (\mathfrak{b}) or head-to-head (\mathfrak{h}) embedding, we can employ standard clustering techniques to partition the ballots. Recall that the Kemeny problem is to find the optimal center of a profile by d_H : that is, the ranking minimizing the summed Kendall tau distance to voters. An algorithm that outputs the minimizer is known as the Kemeny voting rule; this is well known to be NP-hard. Similarly, the 2-Kemeny problem seeks two centers that optimize the total cost, given by summing the distance of voters to the nearer center. Previous authors have recognized the descriptive relevance of these centers. Indeed, Faliszewski et al. [2023] define a polarized election as one better described by two centers than one.

Here, we can make nontrivial use of the metric results to observe that sufficiently polarized elections have canonical clusterings. Recall that d and d' are called 2-biLipschitz equivalent metrics on the same set X if $\frac{1}{2}d'(x, y) \leq d(x, y) \leq 2d'(x, y)$ for all x, y .

Theorem 3.1 (Classification stability). *An (R, r) -polarized election with respect to a distance d on ballots is one for which there are centers x, y with $d(x, y) > R$ and all cast ballots lie within distance r of either x or y . Then if $R > 4r$, any (R, r) -polarized election has a unique optimal clustering. Furthermore, if $R > 10r$, then the same clustering is also optimal with respect to any 2-biLipschitz-equivalent d' .*

Proof. Suppose an election is (R, r) -polarized with respect to d and let x, y be centers that witness the polarization. Then the cost of assigning points in $B_r(x)$ to any center in the ball is at most $2r$, and the cost of assigning them to any center in $B_r(y)$ is at least $R - 2r$. The classification is determined as long as $R - 2r > 2r$. With respect to d' , the within-ball distance is at most $4r$ and the between-ball distance is at least $\frac{1}{2}R - r$, so we need $\frac{1}{2}R - r > 4r$. \square

The bounds $d_B \leq d_H < 2d_B$ (Corollary 2.11) let us apply this to our principal metrics. Clearly, if we weaken the hypotheses by allowing only a share of points to lie in the neighborhoods of fixed centers, we obtain a still-meaningful statement requiring the clusterings to substantially agree.

The coordinate embeddings enable us to use standard heuristic clustering algorithms to find approximate centers. Furthermore, at the scale of Scottish elections, we can certify globally optimal 1-Kemeny centers in all 1070 elections and globally optimal 2-Kemeny solutions in virtually all elections with up to 10 candidates.

The most popular class of clustering methods is k -means, which seeks to minimize the sums of squares of L^2 distances to k centers in \mathbb{R}^n . For instance, Lloyd's algorithm is an iterative method that is computationally lightweight. But the standard cost-minimizing formulation relates to L^1 rather than L^2 distances, suggesting use of the PAM (Partitioning Around Medoids) algorithm, which addresses exactly that minimization problem over candidate centers within the dataset. (That is, in our setting, PAM centers must correspond to ballots that were actually cast in the election.) We can also consider allowing centers to vary over valid ballots, whether chosen by voters or not; and the computationally simplest problem of all would be to simply take coordinatewise medians, which may not correspond to ballots at all.

3.2. Grouping the candidates. Another perspective on the problem is to introduce notions of similarity and dissimilarity on the candidates based on the preference profile. By *slate clustering*, we mean any method that partitions the candidates into k *slates*. If desired, this can be used to induce a partition of the voters into *blocs* by associating each ballot with the slate to which it is (in some sense) closest.

One very reasonable approach is to regard candidates as more similar when they tend to be ranked in closer positions by votes.

Definition 3.2 (Candidate dissimilarity by rank difference). For any candidates $A_i, A_j \in \mathcal{C}$, set

$$D_B(A_i, A_j) := \text{avg}_\sigma |\mathbf{b}(\sigma)_i - \mathbf{b}(\sigma)_j|.$$

The notation D_B for a metric on candidates is used to emphasize that, like d_B as a metric on ballots, this definition is constructed through rank differences. As usual, we can apply this with either pessimistic or averaged convention. If we use the pessimistic convention, then unmentioned candidates all have a rank of zero, so unpopular candidates will be considered highly similar. Depending on the application, this may or may not be desired behavior.

Under the averaged convention, the point $\mathbf{b}(\sigma)$ is the centroid of the set of completions $\bar{\sigma}$ that extend σ to a complete ballot. For most of this paper, we have been content to work with the centroid. For this application, we may learn more by dealing with the whole point cloud.

Definition 3.3 (Candidate dissimilarity with point clouds). For a ballot σ , let $\bar{\sigma}$ be the set of complete ballots that can be reached from σ by a sequence of extensions.

Then for any candidates $A_i, A_j \in \mathcal{C}$, set

$$\bar{D}_B(A_i, A_j) := \text{avg}_\sigma \text{avg}_{\tau \in \bar{\sigma}} |\tau(i) - \tau(j)|.$$

It is clear that D_B is a metric on candidates who receive rankings, but for \bar{D}_B this requires proof.

Proposition 3.4. \bar{D}_B is a metric on the set of candidates.

Proof. Clearly \bar{D}_B is symmetric and positive definite. To verify the triangle inequality, let S denote the set of all completions of all cast ballots with the following redundancy convention. If the ballot σ from a given voter has length k , then the $(m-k)!$ distinct completions of σ will each appear $\frac{m!}{(m-k)!}$ times in S . Thus each voter is represented $m!$ times in S . Notice that $\bar{D}_B(A, B)$ equals the average over all $\tau \in S$ of $|\tau(A) - \tau(B)|$. The triangle inequality follows. \square

Now that we have inter-candidate distances, we can use a variety of methods to group the candidates into slates, and from there to assign corresponding blocs of voters. We will focus on two among many possible methods.

- **Centers.** First cluster the candidates: given k , identify the k candidates as centers that minimize the summed D_B -distances to the centers. The i th slate \mathcal{C}_i includes those candidates closest to center i . This slate embeds in \mathbb{R}^m by applying \mathbf{b} to the generalized ballot $(\mathcal{C}_i, \mathcal{C} \setminus \mathcal{C}_i)$. Now partition the voters by associating each ballot σ to its closest slate point $\mathbf{b}(\mathcal{C}_i)$.
- **Agglomeration.** Agglomerate the candidates with respect to \bar{D}_B and average linkage.² To obtain k slates, stop after the appropriate number of agglomeration steps. Now associate each ballot σ to the slate to which it awards the most Borda points per candidate.

²Agglomerative, or hierarchical, clustering requires a *linkage* choice: single, average, or complete. These merge point clouds successively by looking at their mutual distances as measured by minimum, average, or maximum distance of their constituent points, respectively. An example is carried out below in Figure 10.

The first method is the most in keeping with our primary clustering methods for voters. Since the set of candidates is small, the agglomerative clustering used in the second method is also attractive, because it yields an interpretable sequence of merges starting from the candidates as singletons and ending with a pair of slates.

3.3. Synthetic elections. One challenge for testing clustering methods on real-world data is the lack of ground truth about whether voter behavior was polarized—not finding a good nontrivial clustering can indicate a poor clustering method or an unpolarized election. It is therefore desirable to build a test set of synthetic elections with controlled polarization attributes.

Given $n \in \mathbb{N}$, $p \in (0, 1)$, and a complete ballot $\sigma \in \Omega_m$, we randomly generate a cluster $\mathcal{C}(\sigma, n, p) \subset \Omega_m$ comprised of n complete ballots, each obtained from σ by performing a number of random adjacent swaps that is drawn from the geometric random variable with parameter p , in the style of a Mallows model. In other words, each ballot is obtained via a random walk on the complete portion of the ballot graph starting from σ , with as many steps as a p -weighted coin comes up tails. A higher p value corresponds to a tighter cluster (because the coin lands heads more quickly so the walks are shorter). A simple polarized election can then be formed from two or more such clusters, amounting to a mixed Mallows model. We first consider an election-valued random variable

$$\mathcal{E} = \mathcal{C}(\text{ABCDE}, 300, 0.3) \cup \mathcal{C}(\text{EDCBA}, 700, 0.3) \subset \Omega_5.$$

An instance is shown in Figure 5. Here, we use a standard technique called *multidimensional scaling* (MDS) for the visualization: from the full matrix of pairwise distances between points, we find a low-distortion planar embedding in order to visualize the metric. We will employ MDS for visualization throughout the empirical sections of the paper.



FIGURE 5. MDS plot of the ballots in a synthetic election \mathcal{E} . Ballots marked green were hit from both centers.

All of our modeling choices for 2-clustering the voters pick out the ground-truth clusters in this election, even though the cluster sizes are unbalanced. For example, over several instances of \mathcal{E} and several runs of PAM, the identified centers are always $\{\text{ABCDE}, \text{EDCBA}\}$, with cluster sizes close to $\{300, 700\}$. That is, it finds the correct centers and identifies each ballot with its closest center rather than the site from which it originated. Even though Lloyd’s algorithm for the 2-means problem targets minimal L^2 cost rather than L^1 , it gives clusters that differ by only about 1% from the L^1 clusters.³ The agglomerative method discussed in the previous section yields the reasonable slates $\{\{A, B, C\}, \{D, E\}\}$ and produces voter clusters that differ by only about 4% from the previous ones, with cluster sizes (in one instance of \mathcal{E}) of $\{317, 683\}$.

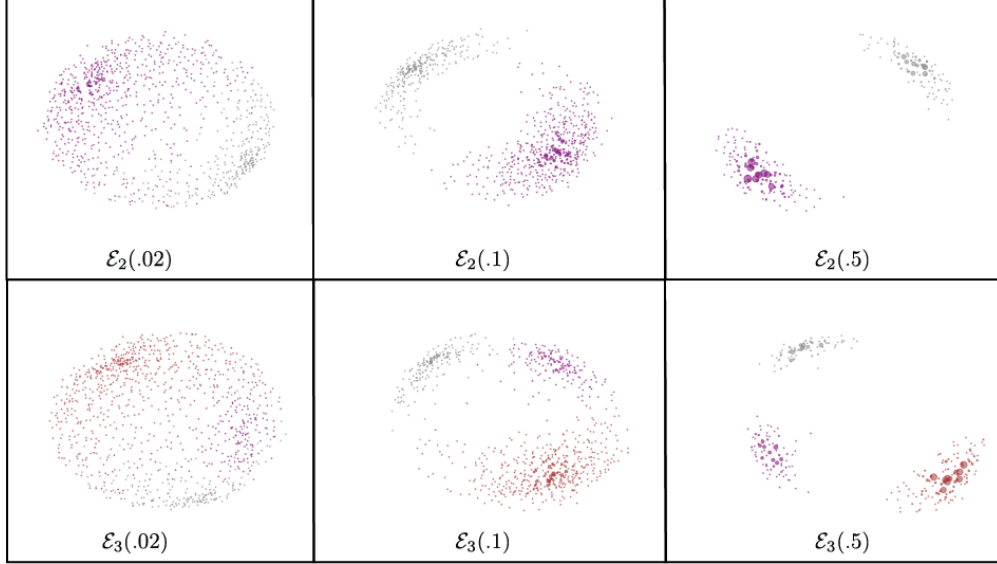
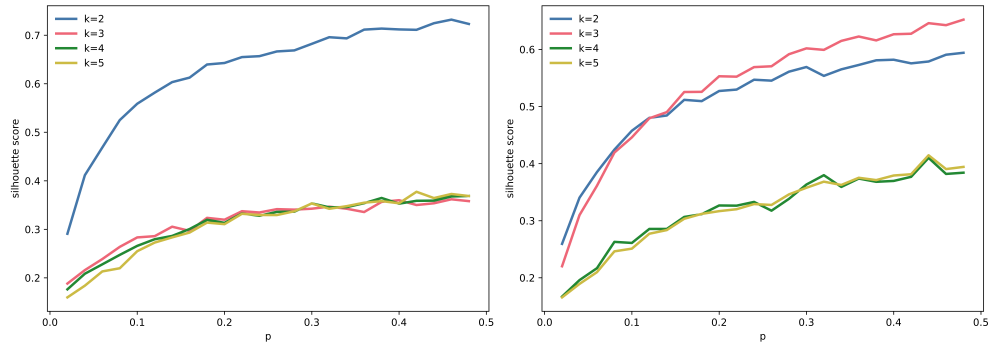
Next, consider 9-candidate elections $\mathcal{E}_2(p)$ and $\mathcal{E}_3(p)$, with instances shown in Figure 6.

$$\mathcal{E}_2(p) = \mathcal{C}(\text{ABCDEFGHI}, 300, p) \cup \mathcal{C}(\text{HGEIFCBAD}, 700, p);$$

$$\mathcal{E}_3(p) = \mathcal{C}(\text{ABCDEFGHI}, 200, p) \cup \mathcal{C}(\text{DFEAHBGCI}, 200, p) \cup \mathcal{C}(\text{HIGDEFBCA}, 600, p)$$

For all values of p between 0.02 and 0.5 by steps of 0.02, the PAM 2-medoids algorithm correctly identified the two centers of $\mathcal{E}_2(p)$ as ABCDEFGHI and HGEIFCBAD. This remained true over multiple runs of PAM

³Two partitions differ by 1% if 1% of the points must be reclassified to convert one partition into the other.

FIGURE 6. MDS plots of the ballots in $\mathcal{E}_2(p)$ and $\mathcal{E}_3(p)$ for three values of p .FIGURE 7. Silhouette scores for Lloyd's k -means clusterings of $\mathcal{E}_2(p)$ (left) and $\mathcal{E}_3(p)$ (right) for values of p from .02 to .5 by steps of .02. (We show k -means instead of PAM clusters for computational efficiency.)

and multiple instances of \mathcal{E} . For *almost all* values of p in this same range, the PAM 3-medoids algorithm correctly identified the three centers of $\mathcal{E}_3(p)$; The only discrepancies occurred with $p = 0.02$ and $p = 0.04$; in some trials with these values, one or two of the medoids were off by a single swap move.

There are several common methods for identifying the "best" choice for the number of clusters in a dataset. One common method is to construct *silhouette scores*, which compare a point's average distance to other points within its cluster against the average distance to points in the nearest other cluster. These are thought to be normalized so that if the silhouette score for the best 3-clustering is larger than the score for the best 2-clustering, it signals that the data is better described by three clusters. Figure 7 shows that this silhouette scores in our synthetic elections. For $\mathcal{E}_2(p)$, the silhouette method clearly picks out two clusters, even at very low values of p . However, for $\mathcal{E}_3(p)$, two or three clusters looks equally apt for $p \leq 0.14$, and better than four or five.

4. RESULTS ON SCOTTISH ELECTIONS

We begin with a detailed walk-through of implementing the clustering methods on a particular (arbitrary) contest from the Scottish local government elections: Edinburgh Ward 2 (Pentland Hills), 2017. From there, we will zoom out to an overview of the whole Scottish dataset.

4.1. Learning voter blocs in Pentland Hills. The Pentland Hills election had seven candidates competing for three seats.

1=Graeme Bruce (Con), 2=Emma Farthing (LD), 3=Neil Gardiner (SNP), 4=Ricky Henderson (Lab), 5=Ernesta Noreikiene (SNP), 6=Susan Webber (Con), 7=Evelyn Weston (Grn).

Here, **Con** is the Conservative and Unionist Party, **LD** is Liberal Democrats, **SNP** is the (ruling, centrist) Scottish National Party, **Lab** is Labour, and **Grn** is the Green Party. These five are the most important players in local government, together holding 1071 out of 1227 seats at the time of writing. Independent candidates, not to be confused with candidates for the Independence for Scotland Party (ISP), also receive significant support.

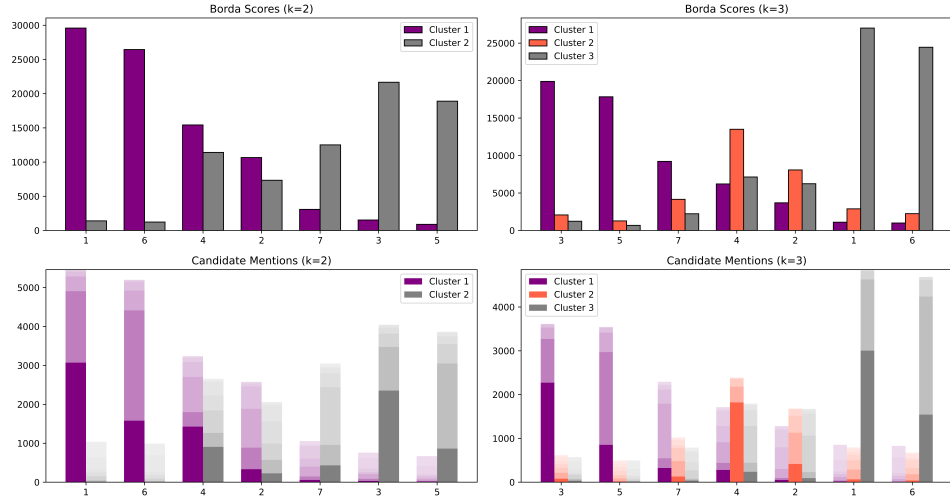


FIGURE 8. Borda plots (top) and mentions plots (bottom) of the optimal k -clusterings using Borda distance with $k = 2$ and $k = 3$. The total height of each bar in a "mentions" plot is the number of ballots in the cluster that ranked the candidate in any position, with first-place rankings represented by the darkest shade and so on.

First, we describe the preference profile. The 11,315 cast ballots in this contest ranged from bullet votes (length 1, occurring 967 times) to complete ballots (length 7, occurring 1431 times). Overall, the average ballot length was 3.2. There are 18 ballots cast over 100 times each, led by the ballot (1,6) ranking the conservatives in alphabetical order and leaving the rest blank—that ballot was cast by 1342 voters, about 11.8% of the electorate. Together, the ones receiving at least 100 votes account for more than half of the votes, but there is an extremely long tail, with 660 ballots receiving exactly one vote. Overall, 1238 different types were cast out of 8659 possible valid ballots.

In Figure 8, we show the global d_B optima for minimizing cost over all ballots for $k = 2$ and $k = 3$. The $k = 2$ solution partitions the voters into two clusters of roughly equal size (6513 in Cluster 1 and 4802 in Cluster 2). The $k = 3$ solution has clusters of size 3798, 2565 and 4955.

Whether we use head-to-head, pessimistic, or averaged Borda, whether we use L^2 or L^1 methods, and whether we require cast-ballot centers, valid ballots, or allow arbitrary centers in coordinate space, we obtain very similar centers and very similar groupings of voters. The $k = 2$ cast-ballot centers (the pair of ballots that minimize the cost) always includes (1,6) as one center. The other center always begins with (3,5) and may be (3,5,7,4), (3,5,7), or (3,5,4) depending on the method. For $k = 3$, all of the embedding choices produce the same centers: (1,6), (3,5,7), (2,4).

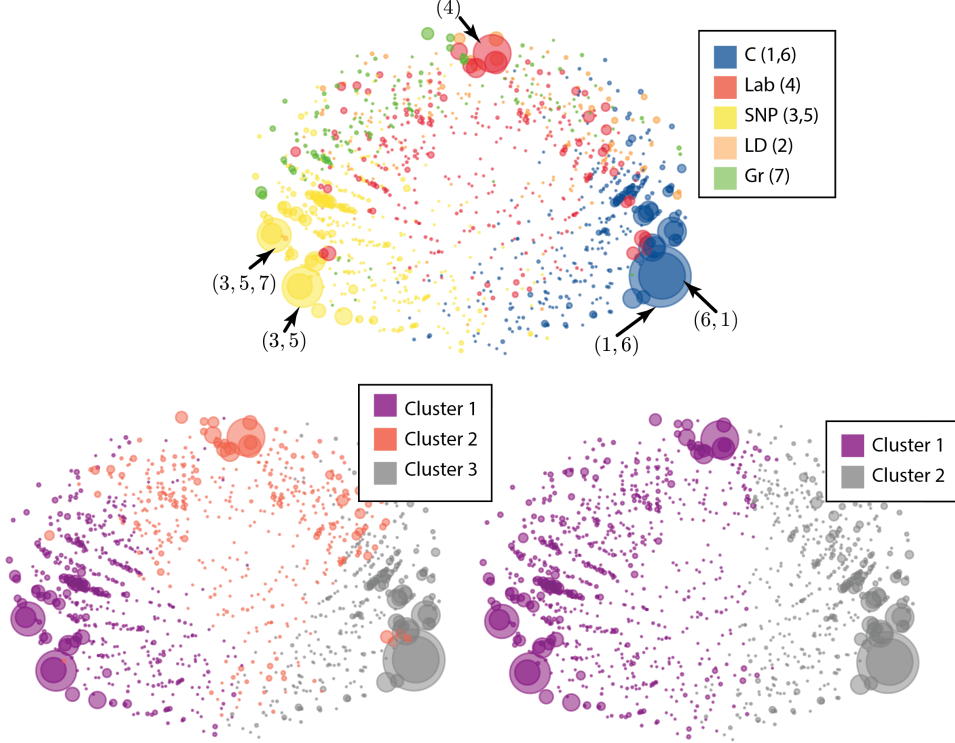


FIGURE 9. Visualization of the ballots in Pentland Hills with respect to 6. All three images use the same low-distortion MDS embedding of the ballots, approximating their d_B distances. Each marker's area is proportional to the number of voters who cast that ballot. In the top plot, the ballots are colored by the party of the first-place vote, and on the bottom they are colored by their cluster assignment for $k = 2$ and $k = 3$ clusters.

What is the right choice for the number of clusters in this Pentland Hills example? Silhouette scores identify $k = 2$. However, the choice $k = 3$ also scores well and is compelling because, as illustrated in Figure 9, the 3-clustering assignments look reasonable and align closely with the party of the first-place vote; that is, the choice $k = 3$ best encodes the SNP–Lab–Con triangle that stands out in the party labeling (Figure 9).

4.2. Learning candidate slates in Pentland Hills. Next, we sort the candidates rather than the voters. As illustrated in Figure 10, the slate clusters are identical whether we use the centers method based on raw rank difference (D_B) or the agglomerative method with ballot completion (\bar{D}_B).⁴ A comparison of Figures 9 and 10 also shows that these inter-candidate differences echo the embedded structure of the full preference profile.

The candidate-centric methods agree that $\{1, 6\}$ is a candidate cluster whether there are two clusters or three. That squares well with the identification of $(1, 6)$ as a ranked ballot appearing as central to blocs across all voter clustering methods in the previous section. One difference is whether the Green candidate (7) is grouped with SNP candidates (3 and 5) or with the Labour/Liberal Democrat candidates (2 and 4). As Figure 10 shows, either choice is close to optimal in the space of candidates.

⁴Switching to complete or single linkage instead of average linkage makes only small changes. At $k = 2$ partition, the slating remains unchanged under all linkage methods. The $k = 3$ partition remains the same using complete linkage, whereas single linkage produces the slates $\{1, 6\}, \{4\}, \{2, 3, 5, 7\}$.

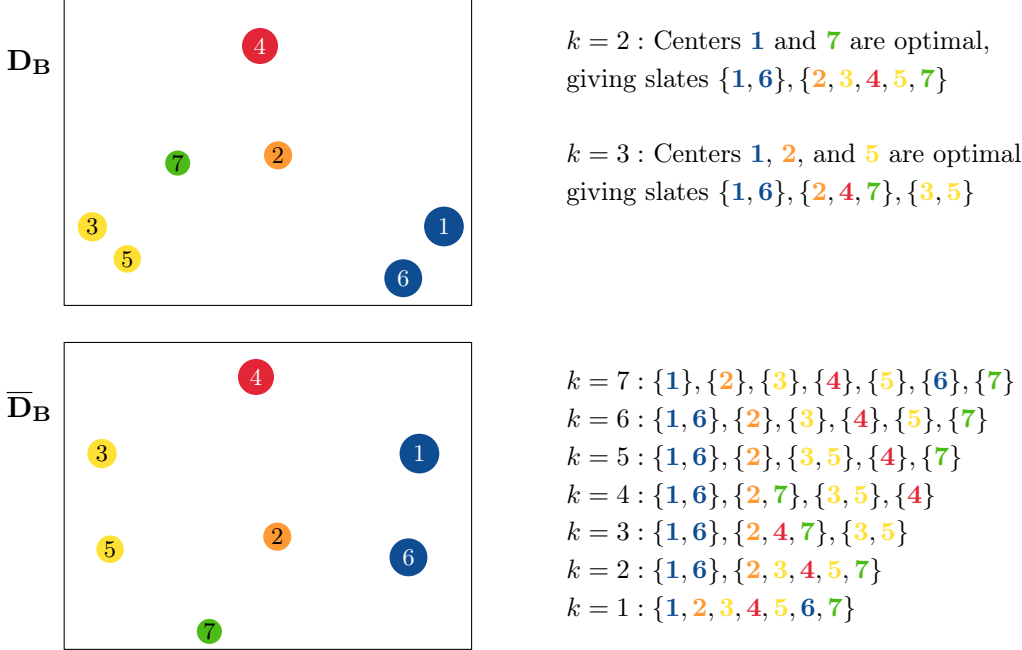


FIGURE 10. MDS plots of the Pentland Hills candidates by D_B and \bar{D}_B , colored by party and sized by the number of mentions received. The optimal centers for D_B slate clustering are shown, as well as the successive steps for agglomerative \bar{D}_B slate clustering. The $k = 2$ and $k = 3$ slates match exactly across the two methods.

4.3. Overview across dataset. To approach clustering on the Scottish dataset, we first compare 2-clustering methods. We can efficiently sweep the dataset with the heuristic methods described above. Then, with integer programming methods described in forthcoming work with David Shmoys and Peter Rock, we can confirm that the heuristic optima are often in fact globally optimal. In over 90% of Scottish elections (981 matches with Borda embeddings and 1010 with head-to-head), the PAM heuristic finds precisely optimal centers. Appendix A offers a fuller discussion of comparison for the approximate methods.

More fundamentally, we can study the degree of agreement of exact optima across methods. To evaluate this, we can start by regarding the center of the whole election as a summary of the preference profile—the minimum-cost cast ballot. For $k = 1$, 74.6% of the elections have matching head-to-head and Borda centers, meaning that the Kemeny rule would give the same output ranking as the Borda median rule, even with partial ballots available. This is notable because Kemeny is strongly Condorcet consistent—if any candidate is preferred head-to-head to all others, they rank first; if any candidate is preferred to all but the first, they rank second, and so on. Rules based on positional scores like Borda count have no such guarantee and are *a priori* very different.

When we pass to optimal pairs under cost-minimization, the exact agreement of centers is significantly more demanding. But for $k = 2$, the degree of agreement is almost as high: 73.5% of the elections have perfectly matching d_H and d_B centers (i.e., both centers agree).

Though our methods for grouping candidates are party-agnostic, we can use party labels as a partial ground-truth validation. Both methods of slate clustering perform well at keeping political parties together. Among the 1070 Scottish elections, 855 of them include more than one candidate from at least one of the five major parties (SNP, Lab, Con, LD, Grn). It is extremely rare (occurring eight times for the centers method and just three for the agglomerative method) for the $k = 2$ slates to split any pairs of candidates from the same party. But beyond recovering parties, we can discover inter-party structure: for instance, the two most consistently close parties across this dataset are the Scottish National Party and the Greens (rather than pairing the ruling SNP party with Labour or Liberal Democrats, as might have been expected).

5. CONCLUSION

Although aggregating rankings is an extremely popular topic in the computing literature, surprisingly little of that work is adapted to the real-world setting of ranked choice elections for political office, where an extension to partial rankings is a practical necessity. First and foremost, this paper develops metric theory that situates ballots, candidates, and slates (or sets of candidates) all in common spaces that admit natural extensions of the Kendall tau and Spearman footrule metrics. This enables the use of coordinate tools, on one hand, and graph/network-based tools, on the other.

Building on this foundation, we give detailed methods for grouping voters into like-minded blocs and for grouping candidates according to voter preference. Bloc and slate identification then unlocks the measurement of key descriptive statistics: to measure the *polarization* of an election, we look at the diffusion of blocs about their centers and the distance between those centers. As a direct consequence of inequalities connecting the principal metrics under study, sufficiently polarized elections must give consistent partitions of voters by either ranking metric. Given blocs and slates, it is now straightforward to assess the *proportionality* of a voting rule by whether the slates receive representation in shares aligned with the sizes of voter blocs.

The techniques developed here broadly enable visualization and hands-on data analysis, while giving a strong foundation for unsupervised techniques to learn structural information about observed elections.

ACKNOWLEDGEMENTS

The authors are pleased to thank David Shmoys, Peter Rock, Chris Donnay, Edith Elkind, and Grant Rinehimer for overlapping collaborations and valuable feedback.

REFERENCES

Elliot Anshelevich, Aris Filos-Ratsikas, Nisarg Shah, and Alexandros A. Voudouris. Distortion in social choice problems: The first 15 years and beyond. In *Proceedings of the Thirtieth International Joint Conference on Artificial Intelligence (IJCAI)*, pages 4294–4301, 2021.

Ludwig M. Busse, Peter Orbanz, and Joachim M. Buhmann. Cluster analysis of heterogeneous rank data. In *Proceedings of the 24th international conference on Machine learning*, page 113–120, Corvalis Oregon USA, June 2007. ACM. ISBN 9781595937933. doi: 10.1145/1273496.1273511. URL <https://dl.acm.org/doi/10.1145/1273496.1273511>.

Burak Can, Alperen I. Özkes, and Ton Storcken. Measuring polarization in preferences. *Social Choice and Welfare*, 44(4):737–755, 2015.

Douglas E. Critchlow. *Metric methods for analyzing partially ranked data*. Lecture notes in statistics. Springer-Verlag, Berlin; New York, 1985. ISBN 9780387962887.

Persi Diaconis and R. L. Graham. Spearman’s footrule as a measure of disarray. *Journal of the Royal Statistical Society Series B: Statistical Methodology*, 39(2):262–268, January 1977. ISSN 1369-7412, 1467–9868. doi: 10.1111/j.2517-6161.1977.tb01624.x. URL <https://academic.oup.com/jrssb/article/39/2/262/7027404>.

Cynthia Dwork, Ravi Kumar, Moni Naor, and Dandapani Sivakumar. Rank aggregation methods for the web. In *Proceedings of the 10th International World Wide Web Conference (WWW 2001)*, pages 613–622, 2001.

Joan-Maria Esteban and Debraj Ray. On the measurement of polarization. *Boston University - Institute for Economic Development*, August 1991. URL <https://ideas.repec.org/p/fth/bosecd/18.html>.

Ronald Fagin, Ravi Kumar, and D. Sivakumar. Comparing top k lists. *SIAM Journal on Discrete Mathematics*, 17(1):134–160, January 2003. ISSN 0895-4801, 1095-7146. doi: 10.1137/S0895480102412856. URL <http://pubs.siam.org/doi/10.1137/S0895480102412856>.

Ronald Fagin, Ravi Kumar, Mohammad Mahdian, D. Sivakumar, and Erik Vee. Comparing partial rankings. *SIAM Journal on Discrete Mathematics*, 20(3):628–648, January 2006. ISSN 0895-4801, 1095-7146. doi: 10.1137/05063088X. URL <http://pubs.siam.org/doi/10.1137/05063088X>.

Piotr Faliszewski, Andrzej Kaczmarczyk, Krzysztof Sornat, Stanisław Szufa, and Tomasz Wąs. Diversity, agreement, and polarization in elections. In *Proceedings of the Thirty-Second International Joint Conference on Artificial Intelligence*, page 2684–2692, Macau, SAR China, August 2023. International Joint Conferences on Artificial Intelligence Organization. ISBN 9781956792034. doi: 10.24963/ijcai.2023/299. URL <https://www.ijcai.org/proceedings/2023/299>.

Peter C. Fishburn. Condorcet social choice functions. *SIAM Journal on Applied Mathematics*, 33(3):469–489, November 1977. ISSN 0036-1399, 1095-712X. doi: 10.1137/0133030. URL <http://pubs.siam.org/doi/10.1137/0133030>.

Hadi Hashemi and Ulle Endriss. Measuring diversity of preferences in a group. In *Proceedings of the 2014 International Conference on Autonomous Agents and Multi-Agent Systems (AAMAS)*, pages 551–558, 2014.

Jonas Israel and Markus Brill. Dynamic proportional rankings. *Social Choice and Welfare*, 2025. Forthcoming.

Eric Kamwa. Scoring rules, ballot truncation, and the truncation paradox. *Public Choice*, 192(1–2):79–97, July 2022. ISSN 0048-5829, 1573-7101. doi: 10.1007/s11127-022-00972-8. URL <https://link.springer.com/10.1007/s11127-022-00972-8>.

Alexander Karpov. Preference diversity: Keeping options open. In *Proceedings of the 26th International Joint Conference on Artificial Intelligence (IJCAI)*, pages 2399–2405, 2017.

Maurice G. Kendall. *Rank correlation methods*. Griffin, London, 4th ed edition, 1970. ISBN 9780852641996.

Maurice G. Kendall and Jean Dickinson Gibbons. *Rank correlation methods*. E. Arnold; Oxford University Press, London: New York, NY, 5th ed edition, 1990. ISBN 9780195208375.

Clemens Puppe. The single-peaked domain revisited: A simple global characterization. *Journal of Economic Theory*, 176:55–80, July 2018. ISSN 0022-0531. doi: 10.1016/j.jet.2018.03.003. URL <https://www.sciencedirect.com/science/article/pii/S0022053118300863>.

Piotr Skowron, Martin Lackner, Markus Brill, Dominik Peters, and Edith Elkind. Proportional rankings. In *Proceedings of the 26th International Joint Conference on Artificial Intelligence (IJCAI)*, pages 409–415,

2017.

Anke Van Zuylen and David P. Williamson. Deterministic pivoting algorithms for constrained ranking and clustering problems. *Mathematics of Operations Research*, 34:594–620, August 2009. ISSN 0364-765X, 1526-5471. doi: 10.1287/moor.1090.0385. URL <https://pubsonline.informs.org/doi/10.1287/moor.1090.0385>.

APPENDIX A. COMPARING HEURISTIC METHODS

Table 1 indicates a high degree of concordance among outputs over our database of 1070 Scottish council elections between 2012 and 2022. In particular, the choice of embedding (\mathfrak{b} or \mathfrak{h}) is generally of fairly mild consequence. Although we did not include in the table, $\mathfrak{b}_{\text{avg}}$ performed very similarly to \mathfrak{b} . Figure 11 (left) uses MDS to visualize the distances reported in the table. Recall that since Lloyd's is solving the L^2 problem, it's giving back the standard Borda ranking (ranking candidates by their total Borda score) while PAM is giving a median in place of an average.

	Lloyd \mathfrak{b}	Lloyd \mathfrak{h}	PAM \mathfrak{b}	PAM \mathfrak{h}
Lloyd \mathfrak{b}	0.00	0.02	0.07	0.07
Lloyd \mathfrak{h}	-	0.00	0.07	0.07
PAM \mathfrak{b}	-	-	0.00	0.04
PAM \mathfrak{h}	-	-	-	0.00

TABLE 1. The average over 1070 elections of the differences between the 2-clustering methods. Each cell represents the portion of ballots in the election for which the two partitions disagree on average. Diagonal cells represent the average disagreement between two runs of the same method. All cells are rounded to 2 decimals.

Next, we compare the results of slate clustering by the two methods emphasized above. To compare the sizes of slates in an apples-to-apples fashion, we restrict to the 282 Scottish elections that have seven candidates (the most common number of candidates). For the separation of candidates into two slates, we report the size of the smaller slate.

- Via centers: 35 slates of size 1, 164 slates of size 2, 83 slates of size 3
- Via agglomeration: 23 slates of size 1, 185 slates of size 2, 74 slates of size 3

Figure 11 (right) shows the distribution of bloc sizes for each 2-clustering method. None of the clustering methods specifically target balanced bloc sizes, but the results in Scotland tend toward balanced blocs for all clustering methods.

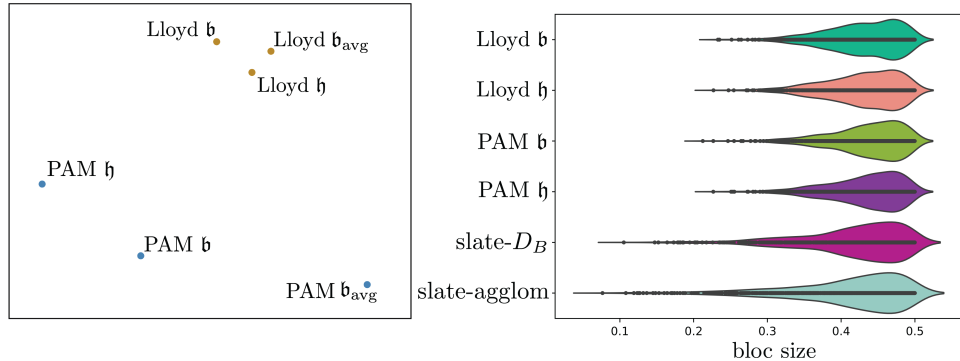


FIGURE 11. LEFT: MDS plot of distances between clustering methods from Table 1. RIGHT: A visualization of how balanced the cluster sizes are in the 2-bloc case. Smaller bloc shown.

APPENDIX B. VISUALIZING POLARIZATION

The agglomerative slates for $k = 2$ and 3 in the Pentland Hills election are pictured in Figure 12 in a way that illustrates the election’s level of polarization with respect to these slates. The idea of this visualization is that the k vertices of the simplex $\Delta^{k-1} = \{(x_1, \dots, x_k) \mid \sum x_i = 1, \text{ all } x_i \geq 0\}$ represent the k slates. Each ballot σ cast in the election has a position $f(\sigma) \in \Delta^{k-1}$ determined so that a ballot is positioned closer to a slate that it more strongly supports, and the plots illustrate the density of the cast ballot images over the simplex. More precisely, we used the function

$$(1) \quad f(\sigma) = \frac{(v_1, \dots, v_k)}{v_1 + \dots + v_k},$$

where v_i is the average number of (pessimistic) Borda points that σ awards to the candidates in the i^{th} slate.

This definition of f is consistent with our agglomerative slate-clustering method of assigning ballots to slates; that is, the agglomerative method was defined to assign each ballot σ to the slate corresponding to the vertex of Δ^{k-1} closest to $f(\sigma)$.

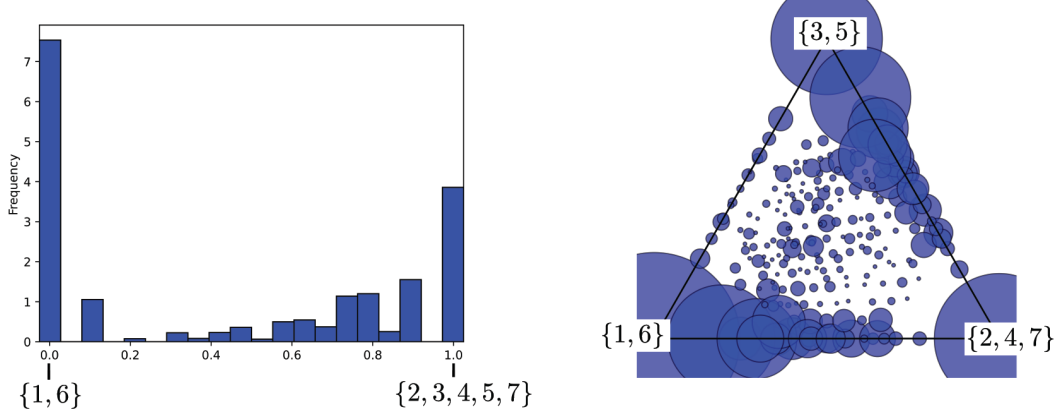


FIGURE 12. Plots showing the density of ballots cast in the Pentland Hills election with respect to the $k = 2$ and $k = 3$ slates obtained from either clustering method. On the right, the triangle represents Δ^2 and the area of each circle is proportional to the number of ballots σ mapped to $f(\sigma)$.

For both $k = 2$ and $k = 3$, the set of slates in Figure 12 arose from agglomerative clustering of the candidates, but it happens to also be the partition of the candidates that minimize the sum over the ballots σ of the Euclidean distance in Δ^k from $f(\sigma)$ to the nearest vertex (slate). In other words, Figure 12 helps to visualize the profile’s level of polarization with the choice of slates maximizing that polarization. This observation suggests another reasonable slate clustering method: directly select the slates that solve this optimization problem. Compared to the agglomerative method, this alternative version is computationally more demanding but yields an interpretable visualization. The two method agree in the Pentland Hills election (because they turn out to yield the same slates, and they use the same method of associating ballots to slates).

DATA SCIENCE INSTITUTE, UNIVERSITY OF CHICAGO
Email address: mduchin@uchicago.edu

DEPARTMENT OF MATHEMATICS, SAINT JOSEPH’S UNIVERSITY
Email address: ktapp@sju.edu